LIMNOLOGY and OCEANOGRAPHY

ASLO

Limnol. Oceanogr. 61, 2016, 1033–1048

doi: 10.1002/lno.10271

Coupled nitrification–denitrification leads to extensive N loss in subtidal permeable sediments

Hannah K. Marchant,*[1] Moritz Holtappels,[1,2] Gaute Lavik,[1] Soeren Ahmerkamp,[1] Christian Winter,[2] Marcel M. M. Kuypers[1]

[1]Biogeochemistry Department, Max Planck Institute for Marine Microbiology, Bremen, Germany
[2]MARUM—Center for Marine Environmental Sciences, University of Bremen, Bremen, Germany

Abstract

We investigated microbial pathways of nitrogen transformation in highly permeable sediments from the German Bight (South-East North Sea) by incubating sediment cores percolated with ^{15}N-labeled substrates under near in situ conditions. In incubations with added $^{15}NH_4^+$, production of $^{15}NO_2^-$ occurred while the sediment was oxic, indicating ammonia oxidation. Similarly, $^{15}NO_3^-$ production during $^{15}NO_2^-$ incubations indicated nitrite oxidation. Taken together these findings provide direct evidence of high nitrification rates within German Bight sands. The production of ^{15}N-N_2 on addition of $^{15}NO_3^-$ revealed high denitrification rates within the sediment under oxic and anoxic conditions. Denitrification rates were strongly and positively correlated with oxygen consumption rates, suggesting that denitrification is controlled by organic matter availability. Nitrification and denitrification rates were of the same magnitude and the rapid production of ^{15}N-N_2 in incubations with added $^{15}NH_4^+$ confirmed close coupling of the two processes. Areal rates of N-transformation were estimated taking advective transport of substrates into account and integrating volumetric rates over modeled oxygen and nitrate penetration depths, these ranged between 22 μmol N m^{-2} h^{-1} and 94 μmol N m^{-2} h^{-1}. Furthermore, results from the ^{15}N-labeling experiments show that these subtidal permeable sediments are, in sharp contrast to common belief, a substantial source of N_2O. Our combined results show that nitrification fuels denitrification by providing an additional source of nitrate, and as such masks true N-losses from these highly eutrophic sediments. Given the widespread occurrence of anthropogenically influenced permeable sediments, coupled benthic nitrification–denitrification might have an important but so far neglected role in N-loss from shelf sediments.

Shallow coastal seas are subject to high loads of anthropogenic inorganic nitrogen inputs from both riverine sources and atmospheric deposition. These inputs cause eutrophication, which has negative impacts on the ecosystem ranging from changes in species composition, increased phytoplankton blooms and bottom water hypoxia (Rabalais 2002). Eutrophication in shallow coastal seas is alleviated by denitrification, which is stimulated by high nitrate and organic matter (OM) inputs. The heterotrophic denitrification that occurs in shallow sediments therefore makes these environments significant hotspots of N-loss in global budgets (Devol et al. 1997; Gruber and Galloway 2008; Gao et al. 2012).

*Correspondence: hmarchan@mpi-bremen.de

Additional Supporting Information may be found in the online version of this article.

Until recently, benthic nitrogen cycling studies were carried out mainly in muddy sediments. However, up to 70% of all continental shelves are comprised of coarse grained sandy sediments (Emery 1968), in which pore water advection can occur (Huettel et al. 2003). Advection transports bottom water into the sediment at timescales up to three orders of magnitude higher than diffusion (Huettel et al. 2003). This supplies the sediment with organic matter and electron acceptors, and furthermore, increases oxygen penetration depths, which oscillate within the sediment dependent on tidal forcing and ripple migration (Huettel et al. 2003; Cook et al. 2007). As a result of advective solute supply, high rates of organic matter mineralization occur in permeable sediments (de Beer et al. 2005), and benthic denitrification rates are among the highest in the marine environment (Gao et al. 2010, 2012). Furthermore, variations in oxygen concentrations appear to stimulate the co-occurrence of aerobic and anaerobic processes, for example denitrification (which is considered to be a predominantly anaerobic process), has

been observed in oxic permeable sediments using diverse experimental set-ups (Rao et al. 2008; Gao et al. 2010; Marchant et al. 2014).

The German Bight is an example of a shallow eutrophied coastal sea, which is dominated by permeable sediments and receives extensive anthropogenic dissolved inorganic nitrogen (DIN) inputs from riverine and atmospheric sources (Van Beusekom 2005; Paetsch et al. 2010). Fluxes of DIN out of the German Bight are lower than the anthropogenic and advective influxes (Beddig et al. 1997; Paetsch et al. 2010), indicating that high levels of benthic N-loss must occur. Furthermore, based on natural abundance stable isotope signatures of nitrate, it has been suggested that intense N-recycling occurs through nitrification, possibly within the sediment (Dähnke et al. 2010).

Benthic N-loss studies in permeable sediments have so far focused on the increased flux of nitrate and organic matter from the water column, therefore little is known about the extent of nitrification. Nitrification has been observed in permeable sediments under diffusive conditions, yet very few, if any, measurements of ammonia oxidation and nitrite oxidation have been undertaken under advective conditions. If occurring, benthic nitrification could provide a secondary nitrate source for denitrification or recycle remineralized N to the environment. The catalytic properties of permeable sediments, which has led to their description as "natural bioreactors" (Huettel et al. 2014) makes nitrification and its subsequent coupling to denitrification likely to occur.

So far however, coupled nitrification–denitrification has rarely been measured directly in eutrophied permeable sediments. In fact in the Wadden Sea nearby the German Bight, the comparatively low ratio of nitrification to denitrification could not support significant amounts of coupled nitrification–denitrification (Marchant et al. 2014). Furthermore, a modeling study has suggested that advection may have a negative impact on nitrification if ammonium generated by remineralization is returned directly to the water column without entering oxic sediment regions (Kessler et al. 2013). In contrast to these findings, coupled nitrification–denitrification has been predicted to occur in permeable sediments from more oligotrophic regions based on isotope pairing studies (Rao et al. 2007, 2008), and sustains N-loss in the Gulf of Mexico when water column nitrate concentrations are low (Gihring et al. 2010). Evidence from permeable bed reactors, which are used frequently in wastewater treatment, also suggests that permeable sediments should foster suitable conditions for coupled nitrification–denitrification. Wastewater treatment has taken advantage of the prevalence of coupled nitrification–denitrification for many decades (Prakasam and Loehr 1972; Sharma and Ahlert 1977); in a process with many parallels to permeable sediments, oxygenated, ammonium rich wastewater is percolated or pumped through permeable media which is colonized with microbes. The ammonium is nitrified and subsequently a switch to anoxic conditions is achieved by increasing the path length of the permeable bed, or intermittently removing the oxygen, where on denitrification occurs (e.g., Yoo et al. 1999; Guo et al. 2005). In simultaneous nitrification–denitrification reactors the spatial or temporal separation of nitrification and denitrification is not even required and the two processes occur while the reactor is oxic (e.g., Münch et al. 1996; Tait et al. 2013).

Studying processes such as coupled nitrification–denitrification in permeable sediments represents a challenge as the advective transport of water and its associated solutes into the sediment must be mimicked. A number of methods have been applied to mimic these conditions, most of which require ex situ incubations. Whole core incubations, in which seawater is percolated into undisturbed sediment were initially used to investigate rates in permeable sediments (Polerecky et al. 2005), however provide low time resolution when optode foils cannot be used (as is the case with N-loss measurements). In recent years however, methods in which sediment is homogenized either in gas-tight bags (Gao et al. 2012), stirred bioreactors (Gao et al. 2010), modified whole cores (Marchant et al. 2014), or flow through columns (Rao et al. 2007, 2008) have been shown to exhibit similar processes (i.e., denitrification in the presence of oxygen has been observed in all), and remarkably similar volumetric rates for the upper few centimeters of permeable sands. The modified whole core method (Marchant et al. 2014) provides increased sampling resolution and allows multiple experiments to be carried out on the same sediment. This is particularly important when investigating detailed relationships between N-cycling processes and when considering the extrapolation of volumetric rates to areal rates. Both of which are required to better understand the role that sandy sediments play in N-loss, especially in highly active eutrophied coastal zones such as the German Bight.

The extent to which nitrification and denitrification might be coupled in sediments is dependent on the availability of ammonium, nitrate, organic matter and oxygen. In permeable sediments the supply of these is determined by advective porewater transport which depends on the physical properties of the sediments (Huettel et al. 2014). Consequently transport-reaction models fueled by measured volumetric rates, sediment characteristics and current speed are required to estimate realistic areal rates.

We investigated the role of nitrification and denitrification in permeable subtidal sediments from the German Bight during summer when water column nitrate concentrations are comparatively low (6–8 μmol L^{-1}). By combining core percolation and ^{15}N labeling experiments we aimed to measure nitrification, dissimilatory N-reduction and their associated N_2O production. Furthermore, we modified a model to take into account both the advective transport of porewater and volumetric rates of interdependent biogeochemical processes; enabling us to extrapolate areal rates of nitrification

and denitrification in this complex flow-dominated system. This allowed us to gain insights into the importance of both organic matter and nitrification in controlling N-loss in subtidal sandy sediments.

Materials and methods

Sediment sampling

Sampling was conducted at three stations in the North Sea around Helgoland on board the RV *Heincke* from 22 June 2012 to 28 June 2012. At each station sediment was collected in a box corer and the top 5 cm were subsampled on deck, homogenized and filled into three PVC cores (height 9 cm, I.D 10.3 cm). Cores were sealed with rubber stoppers fitted with inflow and outflow ports controlled by two way valves. Bottom water was collected using a rosette water sampler and incubations were carried out immediately on board at in situ temperature.

Sediment characteristics

Sub samples of sediment were collected from box cores, transferred to 50 mL falcon tubes (Sarstedt) and returned to Bremen. Porosity was calculated from five replicates by carefully filling a known volume of sediment into volumetric measuring cylinders, ensuring that pore spaces were saturated with water. The weight loss of a known volume of sediment after drying at 60°C was then determined. Grain size distribution was determined on a Beckman Coulter LS Particle Analyzer at the Center for Marine Environmental Sciences (MARUM), University of Bremen and results were analyzed using the GRADISTAT software with the Folk and Ward method as described in Blott and Pye (2001). Permeability of homogenized sediments was measured in triplicate (i.e., sediment columns were repacked between each measurement) using the falling head approach and a setup similar to that described in Rocha et al. (2005).

Sediment core incubations

Nitrogen cycling processes under changing oxygen concentrations (i.e., oxic to anoxic) were determined within percolated sediment cores. The incubations (detailed below) were designed to mimic in situ conditions, where water rich in nitrate, oxygen and organic matter is advected into the sediment and follows curved flow paths. Over time, the air saturated bottom water becomes anoxic and is eventually returned to the water column.

The sampling method, whereby the porewater within the core is rapidly replaced by air saturated, substrate amended water prior to the first time point, captures dynamic conditions in the sediment i.e., the first time point, taken at zero minutes equates to air saturated conditions. Over time, the oxygen concentration in the core drops to below detection limits, and therefore sampling porewater over time from the same core allows measurement of processes first under oxic and then anoxic conditions. As water is sampled regularly, porewater within the core is only stagnant for short periods of time; therefore this method mimics the flow of water through the sediment in a similar way to flow through columns. In this modified version of the percolation method (see Marchant et al. 2014 for further details of the sampling protocol), water is initially replaced by pumping from the bottom of the core and then sampling also takes place from the bottom of the core by letting water flow into Exetainers. This allows greater control than percolating from the top of the core; however is essentially the same principle. Previously we have demonstrated that volumetric rates obtained from the sediment this way are the same as rates using the traditional core percolation method (Marchant et al. 2014).

Volumetric rates of oxygen consumption, ammonia oxidation, nitrite oxidation, denitrification, dissimilatory nitrate reduction to ammonium (DNRA) and anammox were determined at each station in triplicate sediment cores which were percolated with various combinations ^{14}N and ^{15}N inorganic compounds. Four incubations were carried out consecutively on triplicate cores at each station and these are summarized in Table 1. Each incubation was carried out in the same way.

Briefly, bottom water was amended with ^{14}N and ^{15}N inorganic compounds and various inhibitors as appropriate (i.e., NO_3^-, NO_2^- and/or NH_4^+ (see below)). The water was aerated before being pumped upward through the sediment core with a peristaltic pump, exchanging the entire porewater volume in the core with the aerated, N-amended water. After this, porewater was sampled over time from an attachment at the bottom of the core. Six milliliters of porewater was sampled per time point into Exetainers (Labco, High Wickham, U.K.) prefilled with 100 μL saturated $HgCl_2$, taking care to ensure no bubbles were trapped in the Exetainers. Twelve time points were taken between 0 min and 250 min, time points varied per incubation and station and can be seen in Supporting Information Fig. S2.

^{15}N labeling experiments

Incubations were carried out using ^{15}N labeled substrates to determine rates of ammonia oxidation, nitrite oxidation and denitrification, DNRA, anammox and coupled nitrification–denitrification (Table 1). To identify ammonia oxidation rates, $^{15}NH_4^+$ was added to the incubations, as well as pools of $^{14}NO_2^-$ and $^{14}NO_3^-$ ($^{15}NH_4^+ + {}^{14}NO_x$ exp.). These unlabeled pools were added to lower the likelihood that the produced $^{15}NO_2^-$ would be further oxidized to $^{15}NO_3^-$ or reduced to N_2 in subsequent reactions. Similarly, for nitrite oxidation determinations, $^{15}NO_2^-$ was added to the incubations, as well as a pool of $^{14}NO_3^-$. The addition of ^{14}N pools to these incubations would prevent observations of coupled nitrification–denitrification. A further incubation was performed using $^{15}NH_4^+$ and ATU ($^{15}NH_4^+$ + ATU exp). The ATU addition should have inhibited nitrification, however this was not the case (*see* Results and discussion), therefore this

Table 1. Summary of sediment core incubations. Replicates refer to the number of unique sediment cores used for each incubation.

Incubation	Replicates per site	^{15}N amendment (μmol L^{-1})	^{14}N amendment (μmol L^{-1})	Other amendment	Processes targeted
$^{15}NH_4^+$ exp + $^{14}NO_x$	3	NH_4^+ (75)	NO_2^- (100) + NO_3^- (150)	-	Ammonia oxidation
$^{15}NO_2^-$ exp	3	NO_2^- (100)	NO_3^- (150)	-	Nitrite oxidation/reduction
$^{15}NO_3^-$ exp	3	NO_3^- (75)	-	-	Denitrification/DNRA
$^{15}NH_4^+$ + ATU exp.	2	NH_4^+ (75)	-	86 μmol L^{-1} ATU*	Anammox/coupled nitrification-denitrification
$^{15}NH_4^+$ + Acet. exp	1	NH_4^+ (75)	-	10 Pa acetylene†	Anammox

*Allylthiourea was added to block ammonia oxidation to investigate anammox. ATU did not fully block ammonia oxidation so instead this experiment was used to show the close coupling between nitrification and denitrification.
†Acetylene at this concentration fully inhibits ammonia oxidation, but only partly inhibits anammox (Jensen et al. 2007).

experiment was instead used to follow the transformation of ammonium into nitrite, nitrate and N_2 (coupled nitrification–denitrification). To determine whether anammox was present to any significant extent, one core from the low and intermediate permeability stations was incubated with $^{15}NH_4^+$, the ambient background NO_3^- and 10 Pa (4.1 μM) of acetylene ($^{15}NH_4^+$ + acet. exp), at this concentration, acetylene entirely blocks ammonia oxidation, but only partially inhibits anammox (Jensen et al. 2007), therefore any produced $^{29}N_2$ would have originated from anammox. Furthermore, in the denitrification experiment where $^{15}NO_3^-$ was added we compared the labeling percentage ($F^{15}NO_3^{-*}$) (Eq. 1) based on the produced $^{29}N_2$ and $^{30}N_2$ at each time point with the labeling percentage ($F^{15}NO_3^-$) (Eq. 2) from substrate measurements. Deviation between these two values can indicate the occurrence of anammox.

Oxygen determination

Oxygen was determined in each Exetainer using an O_2 microsensor (response time < 2 s), briefly, Exetainers were opened and the microsensor inserted before being closed again. This procedure took less than 5 s and did not result in any water loss from the Exetainers. Oxygen microsensors were constructed as described in Revsbech (1989) and calibration was performed before and after measurements using a 2 point calibration in air saturated seawater and seawater deoxygenated with N_2.

^{15}N analyses

The isotopic N composition of nitrogen and nitrous oxide gas at each time point was determined after replacing 2 mL of water within each Exetainer with a helium headspace. Gas from the headspace was injected directly into a GC-IRMS (VG Optima, Manchester, U.K.), and the isotope ratios of $^{28}N_2$, $^{29}N_2$ and $^{30}N_2$ or $^{44}N_2O$, $^{45}N_2O$ and $^{46}N_2O$ were determined. The concentration of $^{29}N_2$ and $^{30}N_2$ or $^{45}N_2O$ and $^{46}N_2O$ were calculated from the excess of each relative to an air sample or an N_2O sample (Holtappels et al. 2011).

$^{15}NO_2^-$ was determined in subsamples after conversion to N_2 by sulfamic acid. $^{15}NO_3^-$ was determined in a further subsample after NO_2^- removal with sulfamic acid, at which point spongy cadmium was applied to reduce NO_3^- to NO_2^-. After one further sulfamic acid treatment, N_2 was measured from a helium headspace using GC-IRMS as before (Füssel et al. 2011). $^{15}NH_4^+$ was determined in a different set of subsamples after hypobromite oxidation to N_2 (Waremburg 1993; Preisler et al. 2007).

Total nitrate and nitrite determination

The combined concentration of nitrate and nitrite (NO_x) within each Exetainer was determined by a commercial chemiluminescence NO_x analyzer after reduction to NO with acidic Vanadium (II) chloride (Braman and Hendrix 1989). Nitrite was determined after reduction to NO with acidic potassium iodide and nitrate was then calculated by the difference between NO_x and NO_2^-.

Volumetric rate calculations

Volumetric denitrification and DNRA rates were determined during both the oxic part of the incubation (where oxygen was still above 20 μmol L^{-1}) and the anoxic part (where oxygen was below detection limit).

In the $^{15}NO_3^-$ labeling experiment (which was designed to determine denitrification rates), the possibility that anammox had a significant influence on the production of $^{29}N_2$ ($p^{29}N_2$) and $^{30}N_2$ ($p^{30}N_2$) was assessed. The labeling percentage of nitrate was calculated from $p^{29}N_2$ and $p^{30}N_2$, assuming isotope pairing from denitrification only:

$$F^{15}NO_3^{-*} = 2/\left(p^{29}N_2/p^{30}N_2 + 2\right) \quad (1)$$

Values obtained from Eq. 1 were compared at each time point to measured concentrations of labeled and unlabeled nitrate ($F^{15}NO_3^-$)

$$F^{15}NO_3^- = {}^{15}NO_3^-/({}^{14}NO_3^- + {}^{15}NO_3^-) \quad (2)$$

As no significant difference was observed, denitrification rates were then calculated as D_{tot} according to Nielsen (1992).

DNRA rates were determined from the labeling percentage of nitrate (1) and the production of $^{15}NH_4^+$ ($p^{15}NH_4^+$):

$$DNRA = p^{15}NH_4^+ / F^{15}NO_3^{-*} \quad (3)$$

Ammonia oxidation rates were determined from the production of $^{15}NO_2^-$ during the oxic part of the incubations. A pool of $^{14}NO_2^-$ was added to the incubations to prevent further oxidation of $^{15}NH_4^+$ to $^{15}NO_3^-$. In some cases this can be insufficient; leading to the formation of a small amount of $^{15}NO_3^-$, in such cases the $^{15}NO_3^-$ concentration was added to the $^{15}NO_2^-$ concentration before rate determination. Furthermore, during ammonia oxidation the pool of $^{15}NH_4^+$ can become significantly diluted with $^{14}NH_4^+$ formed during remineralization of organic matter. Therefore to avoid rate underestimations we corrected the produced $^{15}NO_2^-$ for the labeling percentage of ammonium at each time point (4).

$$NO_{2tx} = \left(^{15}NO_{2tx} - ^{15}NO_{2tx-1}\right)/(F_{NH4tx} + F_{NH4tx-1})/2 \quad (4)$$

where tx refers to the time point and F_{NH4} is the labeling percentage of ammonium determined by GC-IRMS. Ammonia oxidation rates were then calculated by the increase of NO_{2tx}^- over time.

Nitrite oxidation rates were determined during the oxic part of the incubation from the production of $^{15}NO_3^-$ ($p^{15}NO_3^-$) after addition of $^{15}NO_2^-$. Due to sample limitations we did not correct these rates for changes in labeling percentage.

The amount of ammonium released during oxic respiration was compared with ammonia oxidation rates from ^{15}N-labeling experiments (assuming Redfield stoichiometry of organic matter). Briefly, aerobic respiration of organic matter with a Redfield stoichiometry would lead to production of NH_4^+ at a ratio of 106 O_2/16 NH_4^+;

$$(CH_2O)_{106}(NH_3)_{16}H_3PO_4 + 106O_2 + 16H^+ \rightarrow 106CO_2 + 16NH_4^+ + 106H_2O + H_3PO_4 \quad (5)$$

The oxygen consumed by ammonia oxidation and nitrite oxidation was calculated according to:

$$NH_4^+ \text{ oxidation OCR: } NH_4^+ + 1.5O_2 \rightarrow NO_2^- + H_2O + 2H^+ \quad (6)$$

$$NO_2^- \text{oxidation OCR: } NO_2^- + 0.5O_2 \rightarrow NO_3^- \quad (7)$$

This oxygen consumption was subtracted from total oxygen consumption rate (OCR) to determine potential heterotrophic OCR (Eq. 8). It should be noted however that the remaining OCR may still have been influenced by other autotrophic respirations.

$$\text{Heterotrophic OCR} = \text{Total OCR} - (NH_4^+ \text{ oxidation OCR}) - (NO_2^- \text{ oxidation OCR}) \quad (8)$$

All rates were determined from linear regressions of at least four time points, results of which are given in Supporting Information Table S1.

O_2 and NO_3^- penetration depths and areal rates

Porewater concentrations of O_2 and NO_3^- were not measured during this cruise. In sediments where oxygen availability is controlled by advective fluxes, removing the sediment from the advective system could lead to underestimations in oxygen penetration depth. Additionally, porewater profiles of nitrate are of low resolution in permeable sediments (1–2 cm intervals) due to their low porosity. When nitrification is coupled to denitrification and the processes overlap spatially, precise penetration depths are essential to determine areal rates. Therefore, we took a modeling approach, which allowed us to estimate penetration depth by combining volumetric rates with advectively driven porewater transport. O_2 and NO_3^- penetration depths were derived from a transport model published by Elliott and Brooks (1997a,b), which investigated advective mass transport into permeable sediment as a function of time. The model allows for calculation of an "effective mean mixing depth," from the integral of the residence time function of a solute, which is pumped into the sediment due to the interaction of bottom water currents and seabed topography (ripples). The model does not cover the full complexity found in situ, as diffusion and dispersion are neglected, both of which would lead to an additional transport into deeper sediment layers and increase benthic net fluxes. Therefore, the model approach used here represents a conservative estimate.

For stationary ripples with a simplified geometry Elliott and Brooks (1997b) derived an analytical solution to describe the increase of the effective mean mixing depth (D) of a solute as a function of time (t) after the initial appearance of the solute in the bottom water (Eq. 9).

$$D = 1/k \ln(0.42\, k^2 K h_m\, t/\theta + 1) \quad (9)$$

where K and θ are the measured hydraulic conductivity (in m/s) and porosity, respectively, and k is the wave number ($k = 2\pi/\lambda$) of the ripple length (λ in m). A dynamic hydraulic head (h_m) of 4×10^{-4} m was calculated from measured mean bottom water currents (20 cm/s) and assumed ripple dimensions (height: 2 cm; length: 13 cm; similar to observations made during a subsequent cruise in the same region) using the empirical expression in Elliott and Brooks (1997b, Eq. 28 therein).

The effective mean mixing depth (D) is a parameter based on the residence time function, which includes both, the vertical and horizontal velocity components of porewater flow (*see* Elliott and Brooks 1997b). Two-dimensional (2D) flow patterns as described in many publications (e.g., Thibodeaux and Boyle 1987; Huettel et al. 1996) are thus the basis of the model and are therefore fully considered in our calculation. This is reflected by the non-linear relation between effective mean mixing depth and time in Eq. 9.

In detail, the effective mean mixing depth of O_2 was determined as follows: the time of O_2 depletion from bottom water entering the pore space was calculated from the initial O_2

Table 2. Station locations within the German Bight and water characteristics.

Site	Lat. N	Long. E	Depth (m)	Bottom water temp. (°C)	Air temp. (°C)	Salinity	Bottom water NO_3^- (μM)
1	54° 10,16′	7° 59,70′	21.0	12.9	14.1	32.1	6
2	54° 10,55′	7° 57,24′	23.3	13.2	12.8	31.5	8
3	54° 14,36′	7° 51,31′	18.4	12.8	12.6	32.0	7

Table 3. Sediment characteristics.

Site	Porosity (±SD)	Mode/geometric mean (μm)	Sorting (σ)	Skewness (sk)	Permeability (± SD) (10^{-11} m^2)	Sediment type
1	0.36 (±0.002)	430/440	1.37	−0.02	2.16 (±0.08)†	Well sorted medium sand
2	0.40 (±0.005)*	568/579	1.51	−0.12	4.09 (±0.47)†	Moderately well sorted coarse sand
3	0.36 (±0.001)	430/494	1.57	0.284	6.47 (±0.23)†	Moderately well sorted coarse sand

*Denotes that value is significantly different from other stations in pairwise comparisons (p-value < 0.05 (one-way anova)).
†Denotes that value is significantly different from other stations in pairwise comparisons (p-value < 0.05 (one-way anova)).

Table 4. Mean areal oxygen and N-cycling rates in three permeable sediments in the German Bight determined using the Elliot and Brooks model.

	Oxygen consumption	Nitrification	Denitrification	DNRA
	(mmol m^{-2} d^{-1} ± SD)			
Lower perm. st.	26.3 ± 1.3	1.15 ± 0.7	0.87 ± 0.1	0.02 ± 0.005
Int. perm. st.	49.6 ± 1.0	0.21 ± 0.05	2.28 ± 0.3	0.25 ± 0.05
Higher perm. st.	33.7 ± 2.1	2.98 ± 0.42	0.52 ± 0.03	0.11 ± 0.06
p-value*	<0.001	0.006	<0.001	0.013

*One way ANOVA.

concentration in the bottom water divided by the O_2 consumption rate per volume porewater assuming zero order kinetics. Thereafter the time of depletion was inserted into Eq. 9 to estimate the effective mean mixing depth of O_2. The effective mean mixing depth of NO_3^- was calculated in a similar way. Here, the volumetric rates of nitrification, denitrification and DNRA and their dependence on O_2 concentrations were considered to calculate the time of NO_3 depletion and the NO_3^- mixing depth. To estimate areal rates, the rates per volume sediment were integrated over the mixing depth of the limiting substrate, i.e., O_2 consumption, nitrification, oxic denitrification and oxic DNRA were integrated down to the O_2 penetration depth, and anoxic denitrification and anoxic DNRA were integrated from below the oxycline down to the NO_3^- penetration depth.

To validate the Elliot model, oxygen fluxes and areal N-loss rates from the lower permeability station were compared with a 2D numerical model which includes dispersion, diffusion, and a pressure distribution along a true bedform topography derived from Large-Eddy-Simulations (Ahmerkamp et al. 2015). Volumetric nitrification rates as well as aerobic and anaerobic denitrification rates were added to the transport reaction equations in the Ahmerkamp model and a monod kinetic was assumed for each, where the half saturation co-efficient was kept constant at 1/8 of the bottom water concentration of the respective solutes.

Results

Sediment characteristics and volumetric oxygen consumption rates

Experiments were carried out at three stations in the German Bight (Table 2); all three sites consisted of permeable sands which had significant differences in permeability, grain size and porosity (Table 3). St. 1 had the lowest permeability and was comprised of well sorted medium sand (Supporting Information Fig. S1), hereafter it is referred to as the lower

permeability station. St. 2 had higher permeability and was comprised of moderately well sorted coarse sand, although it had an additional fine sand fraction leading to a fine skew. It is hereafter referred to as the intermediate permeability station. St. 3 had the highest permeability, and was comprised of moderately well sorted medium sand, however there was a coarse skew toward coarse grained sand which would have been greater if an additional fraction of shell fragments and gravel (> 2 mm) had not been removed before analysis on the particle counter. This station is hereafter referred to as the higher permeability station. Total volumetric oxygen consumption rates differed significantly between each station ($p < 0.001$) (Fig. 1). The highest rates (as calculated from the slope of the initial decrease in oxygen) were observed at the intermediate permeability station (268.5 ± 36.5 SD mmol $m^{-3}_{sediment}$ h^{-1}), followed by the lower permeability station (149.2 ± 41.5 SD mmol $m^{-3}_{sediment}$ h^{-1}), the lowest oxygen consumption rates were observed at the higher permeability station (60.2 ± 16.5 SD mmol $m^{-3}_{sediment}$ h^{-1}).

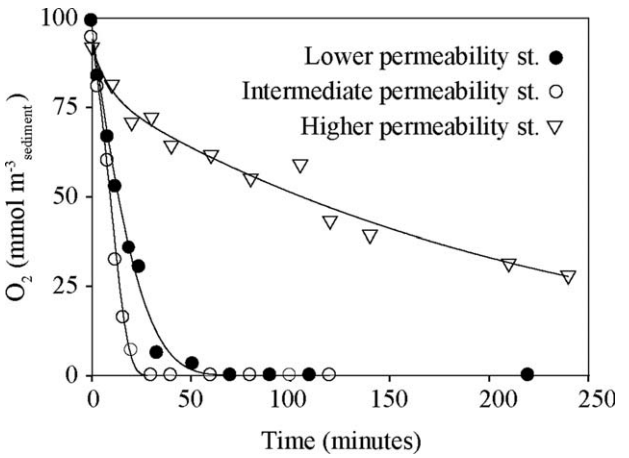

Fig. 1. Examples of oxygen consumption profiles measured during the $^{15}NH_4^+$ addition experiment at all three stations.

Ammonia oxidation

Production of $^{15}NO_2^-$ in the presence of oxygen indicated that ammonia oxidation occurred at all three stations ($^{15}NH_4^+ + {}^{14}NO_x$ exp.; Supporting Information Fig. S2; Supporting Information Table S1). Volumetric ammonia oxidation rates differed significantly between the stations ($p = 0.004$) were highest at the lower permeability station and lowest at the intermediate permeability station (Fig. 2a).

Nitrite oxidation

In the presence of oxygen, production of $^{15}NO_3^-$ occurred after addition of $^{15}NO_2^-$ all three stations ($^{15}NO_2^-$ exp; Supporting Information Fig. S2; Supporting Information Table S1). Volumetric nitrite oxidation rates calculated from the $^{15}NO_3^-$ production decreased from the lower permeability station to the higher permeability station; however there was no significant difference between the stations. Volumetric nitrate oxidation rates were always higher than ammonia oxidation rates, significantly so at the intermediate and higher permeability stations ($p = < 0.002$) (Fig. 2a) and there was a weak but significant positive correlation between the two processes ($r^2 = 0.48$, $p = 0.04$).

Denitrification, anammox, and DNRA

Dissimilatory nitrate reduction processes were determined after the addition of $^{15}NO_3^-$. $^{29+30}N_2$ production occurred at all three stations even when oxygen was present ($^{15}NO_3^-$ exp.

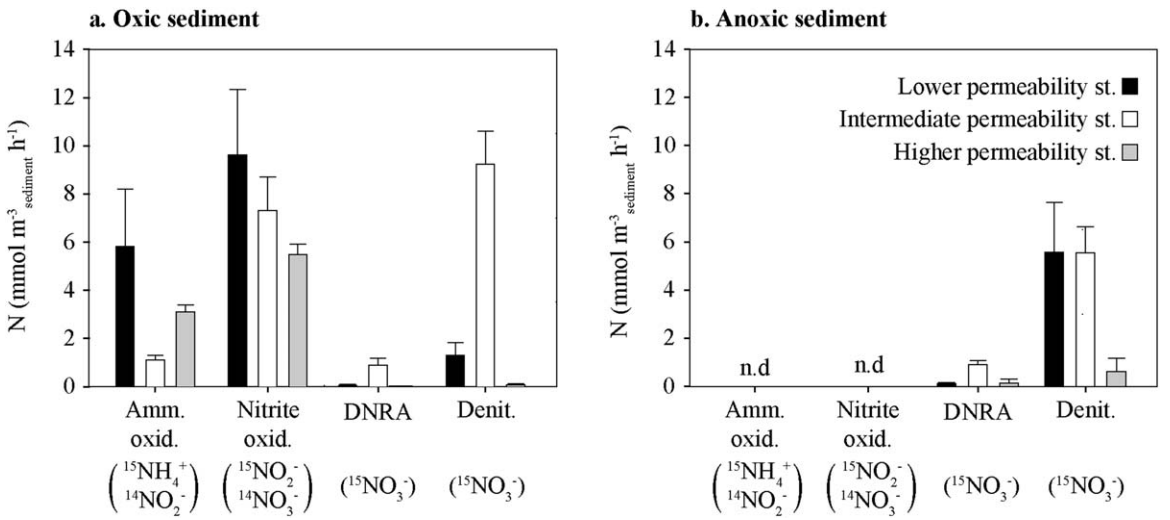

Fig. 2. Volumetric rates of nitrogen cycling processes at all three stations, determined from the (**a**) oxic and (**b**) anoxic phase of the incubation. Substrate additions are shown in brackets in the axis legend, for further details see Table 1. Error bars are SD, $n = 3$ ($n = 2$ at St. 3, $^{15}NO_3^-$ addition experiment) n.d. = not detected.

Supporting Information Fig. S2; Supporting Information Table S1). This was determined to be a result of denitrification, as there was no conclusive evidence of anammox in any experiment (SI text). At the lower and higher permeability station, volumetric denitrification rates increased when the sediment became anoxic (Fig. 2b). At the intermediate permeability station, oxic denitrification rates were high in contrast to the other stations and on anoxia the denitrification rate did not increase. As a consequence of the high oxic denitrification rates at the intermediate permeability station, NO_3^- concentrations were already low when the sediment became anoxic ($\sim$ 10 μmol L^{-1}) and dropped to below detection limit by the time the incubations were terminated. Therefore, we assume that anoxic denitrification rates were most likely substrate limited and thus underestimated. Hence when comparing oxygen consumption rates and denitrification rates we used the anoxic denitrification rates from the higher and lowest permeability stations and oxic rates from the intermediate permeability station. When these denitrification rates were compared with the OCR, there was a significant positive correlation ($p = 0.002$, $r^2 = 0.83$ (Fig. 3)).

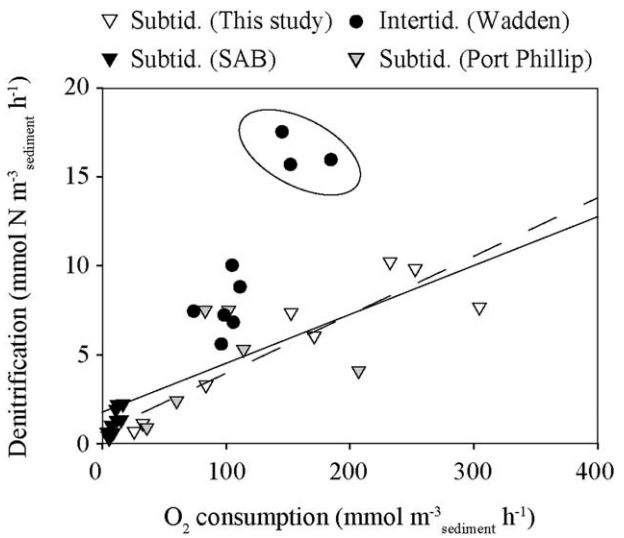

Fig. 3. The correlation between oxygen consumption rates and denitrification rates in a variety of permeable sediments. The dashed line represents the correlation of rates from this study (Total OCR was used) ($p = 0.002$, $r^2 = 0.83$). The solid line represents of the correlation of all points ($p = < 0.001$, $r^2 = 0.37$), excluding the three circled points which represent rates measured during winter in the Wadden Sea, when nitrate concentrations in the water column were on average 70 μmol L^{-1}; which is significantly higher than that at the other time points and locations. The subtidal data from the SAB (South Atlantic Bight) are taken from Rao et al. (2008), subtidal (Port Phillip) refers to the data in Evrard et al. (2013) and the intertidal (Wadden) is from Marchant et al. (2014).

In the $^{15}NO_3^-$ addition experiment the production of $^{15}NH_4^+$ was also observed at all three stations, indicative of DNRA ($^{15}NO_3^-$ exp; Supporting Information Fig. S2). Volumetric DNRA rates were low compared with denitrification (< 20%) but generally showed similar trends (Fig. 2). Similar to denitrification rates, DNRA rates were positively correlated to oxygen consumption rates (Supporting Information Fig. S3).

Coupled nitrification–denitrification

86 μmol L^{-1} allylthiourea (ATU) was added to one set of incubations with the intention of inhibiting nitrification ($^{15}NH_4^+$ + ATU exp.). However, in this experiment, nitrification still occurred and instead, coupled nitrification–denitrification was observed. $^{15}NH_4^+$ was sequentially oxidized to $^{15}NO_2^-$ then $^{15}NO_3^-$, and $^{29+30}N_2$ production began almost immediately (Fig. 4). The sum of all ^{15}N labeled products ($^{15}NO_2^-$,$^{15}NO_3^-$, $^{29+30}N_2$) increased constantly over the first 60 min of the incubation, until O_2 was depleted. At this point $^{15}NO_2^-$ and $^{15}NO_3^-$ concentrations decreased, while ^{15}N-N_2 concentrations continued to increase. The successive increase and decrease of $^{15}NO_x$ coupled to the continuous

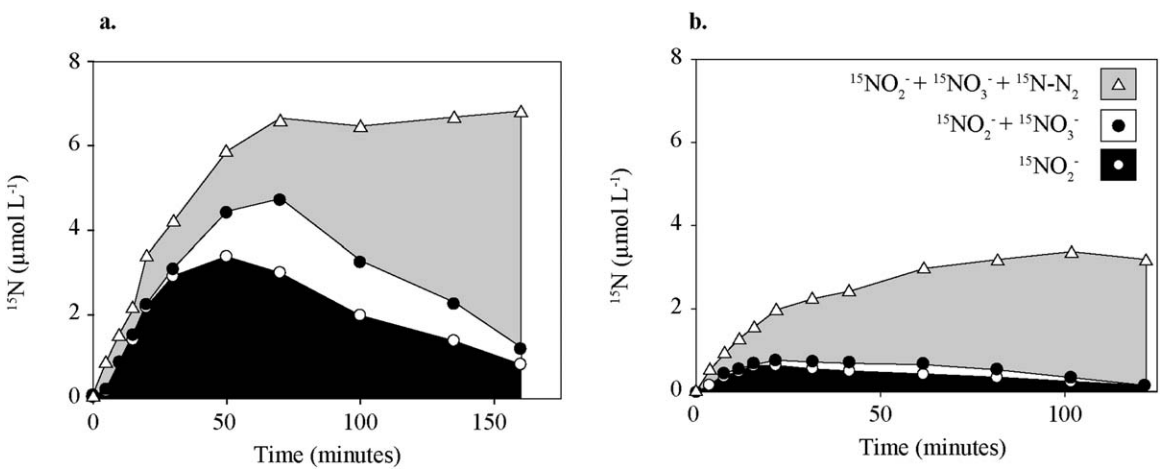

Fig. 4. Evidence for coupled nitrification–denitrification. Stacked area plot of the production of ^{15}N-labeled after $^{15}NH_4^+$ and ATU addition. (**a**) Example from the lower permeability station, (**b**) example from the intermediate permeability station.

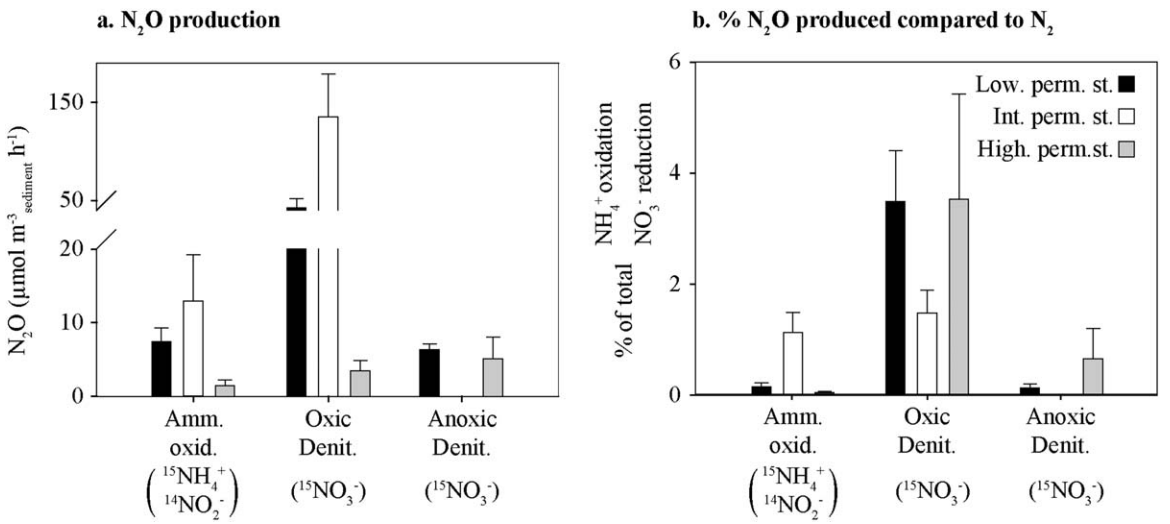

Fig. 5. N_2O formation (**a**) rates of N_2O formation from ammonia oxidation and denitrification. (**b**) N_2O formation rates compared with total ammonia oxidation and denitrification rates. Substrate additions are shown in brackets in the axis legend, for further details see Table 1. Error bars are SD, $n = 3$ apart from anoxic rates at the high permeability station in the $^{15}NO_3^-$ addition experiment, where $n = 2$.

increase of ^{15}N-N_2 (Fig. 4, Supporting Information Fig. S4) indicate close coupling of nitrification and denitrification. Coupled nitrification–denitrification also appeared to be occurring in the $^{15}NO_3^-$ addition experiment. Here the labeling percentage of NO_3^- ($F^{15}NO_3^{-*}$) dropped by 27 (± 1 SD) % at St. 1 during the oxic part of the incubation, suggesting that the $^{15}NO_3^-$ pool added at the start of the incubation was constantly diluted by the production of $^{14}NO_3^-$ via nitrification.

Nitrous oxide (N_2O) production

15N-N_2O formation occurred at all three stations in both the $^{15}NH_4^+$ addition and the $^{15}NO_3^-$ addition experiments ($^{15}NH_4^+ + {}^{14}NO_x$ exp.; $^{15}NO_3^-$ exp. respectively; Supporting Information Fig. S2). In the $^{15}NO_3^-$ addition experiment, the production of $^{45+46}N_2O$ occurred both in the presence and absence of oxygen at the lower and higher permeability stations. There was no difference between volumetric oxic and anoxic N_2O production rates at the higher permeability station ($p = 0.5$), whereas at the lower permeability station N_2O production rates were significantly higher under oxic conditions ($p = 0.05$) (Fig. 5). At the intermediate permeability station, N_2O was only produced under oxic conditions. Despite these differences, the ratio of produced N_2O: N_2 was always significantly higher during the oxic part of the incubations ($p = 0.002$) (Fig. 5b), this resulted from either higher oxic N_2O production rates and/or lower oxic denitrification rates in comparison to anoxic rates. There was little to no net N_2O consumption observed at any point in the $^{15}NO_3^-$ addition experiments at the lower and higher permeability stations, whereas at the intermediate permeability station (where we observed comparatively high oxic denitrification rates), N_2O was produced rapidly at the beginning of the incubation and consumed when the sediment became anoxic and nitrate was depleted ($^{15}NO_3^-$ exp-N_2O; Supporting Information Fig. S2).

O_2 and NO_3^- penetration depths and areal rate estimates

To integrate volumetric rates into areal rates, the transport model of Elliott and Brooks (1997a,b) was applied. To determine nitrate and oxygen concentrations within the sediment along a flow path, we combined the volumetric nitrification rates from the $^{15}NH_4^+ + {}^{14}NO_x$ amendment exp. with the oxygen consumption, denitrification and DNRA rates from the $^{15}NO_3^-$ amendment experiments. Two different scenarios were identified by combining the rate measurements with the bottom water nitrate concentration, one for the lower and higher permeability station and one for intermediate permeability station (upper panels; Supporting Information Fig. S6). At the lower and higher permeability stations, under oxic conditions, the production of nitrate via nitrification exceeded nitrate removal by denitrification and DNRA. Therefore, while oxygen was present, nitrate concentrations increased within the sediment. When oxygen concentrations reached zero, nitrate concentrations had increased from 6 μmol L^{-1} and 7 μmol L^{-1} (bottom water concentration) to 8.9 μmol L^{-1} and 11.8 μmol L^{-1} for the lower and higher permeability station respectively. When oxygen was entirely consumed, the rates of denitrification and DNRA increased and prevailed until nitrate was entirely respired. At the intermediate permeability station while the sediment was oxic the respiration of nitrate by denitrification and DNRA exceeded the production of nitrate by nitrification. Therefore by the time that oxygen concentration

reached zero, nitrate concentration had decreased from 8 μmol L^{-1} (bottom water concentration) to 4.4 μmol L^{-1}.

The effective mixing depths as calculated from the model were 7.5 mm and 12.2 mm for the lower permeability station, 7.7 mm and 11.1 mm for the intermediate permeability station, and 30 mm and 52 mm for the higher permeability station, for O_2 and NO_3^-, respectively (Supporting Information Fig. S6; middle panels). These effective mean mixing depths were used to integrate volumetric rates of oxygen respiration, nitrification, denitrification, and DNRA over specific depth layers. From this integration we derived areal rates of denitrification, nitrification, DNRA and oxygen respiration for all three stations (Table 4).

The oxygen fluxes and areal N-loss rates predicted by the Elliot model were compared with a 2D numerical model from Ahmerkamp et al. (2015). For a parameterization based on the lower permeability station, the Elliot model was highly accurate and underestimates fluxes by only up to 10% for bottom water velocities ranging from 0.05 m s^{-1} to 0.5 m s^{-1}. For example, using a bottom water velocity of 0.2 m s^{-1} (as in the Elliot model) the Ahmerkamp model gave an areal O_2 flux of 28.1 mmol m^{-2} d^{-1} and an areal N-loss rate of 0.95 mmol m^{-2} d^{-1}.

Discussion

N-loss in highly permeable sediments

Subtidal coastal sediments are often sites of anthropogenically induced eutrophication and as such, it is important to understand how they might remove or recycle anthropogenic N-inputs. In temperate coastal waters, nitrate concentrations are generally low in periods when primary production is high (Van Beusekom et al. 2009) and consequently sedimentary nitrification could be an essential but so far understudied source of nitrate for denitrification. Here, we investigated three sediments which have permeabilities representative of the sands which cover approximately 60% of the German Bight (Janssen et al. 2005). By comparing these results to the growing number of observations in diverse other permeable sandy sediments, it is now becoming possible to recognise shared traits between them.

We found that anoxic denitrification was the major N-loss pathway within the highly permeable subtidal German Bight sediments (Fig. 2). This is in line with other studies of sandy sediments, whether they be from subtidal regions with lower permeability (Rao et al. 2008) or from intertidal regions (Gao et al. 2012; Marchant et al. 2014). Despite all three sediments studied here being highly permeable, the variation in volumetric oxygen consumption rates (OCR) and denitrification rates between stations was greater than the variation between replicates from the same station (Supporting Information Table S1). This suggests that differences in permeability, even at values above 10^{-11} m^2 have an effect on biogeochemical processes.

There was a strong correlation between OCR and denitrification (Fig. 3). This correlation is not surprising as OCR is a robust proxy for the amount of labile organic matter in sediments (Glud 2008). When volumetric denitrification rate data from studies on different permeable sediments—subtidal, intertidal, eutrophic and oligotrophic—are taken together, the strong positive correlation between volumetric OCR and denitrification rates persists (Fig. 3); clearly indicating that denitrification potential is controlled by organic matter availability. This suggests that the differences in denitrification observed previously between intertidal and subtidal sandy sediments are not related to the tidal regime itself, but rather to the availability of labile organic matter within the sediment. Intriguingly, when water column nitrate concentrations and OCR are both high, denitrification rates increase more steeply (circled points, Fig. 3), indicating that nitrate concentrations are a secondary controller of denitrification in permeable sediments. These relationships between volumetric OCR, nitrate and denitrification rates may allow better prediction of denitrification rates in sandy sediments. Generally increases in permeability are observed to lead to higher rates (Huettel et al. 2014); however this trend might not persist at very high permeabilities, as indicated by the comparatively low rates we observed at the most permeable station.

The average ratio between OCR and denitrification in our study is about 0.03 and well in line with previous results (Rao et al. 2008; Gao et al. 2010; Evrard et al. 2013; Marchant et al. 2014). This suggests that the relative contribution of denitrification to carbon remineralization is lower in permeable sediments than in cohesive sediments that are generally dominated by sulfate reduction (Jørgensen 1982; Thamdrup and Canfield 1996). While the overall denitrification rates were inefficient relative to oxygen consumption, they were generally higher than those in cohesive sediments, and as such seem to be more important for nitrate removal in coastal environments.

Anammox can significantly contribute to N-loss from sediments with low organic carbon content (Thamdrup and Dalsgaard 2002; Sokoll et al. 2012; Song et al. 2013), however our combined results from the $^{15}NH_4^+$ + acetylene exp. and the $^{15}NO_3^-$ labeling exp. indicate that anammox was not substantial (see SI text for further details). The predominance of denitrification over anammox in sandy sediments from many differing locations (Canion et al. 2014) likely results from the enhanced supply of organic matter by advection and the highly fluctuating oxygen conditions, both of which would favour denitrification.

DNRA also occurred in all three of the sediments; however it made up a relatively small proportion of the total volumetric NO_3^- reduction (DNRA + Denitrification); accounting for 2%, 10%, and 17%, for the lower, intermediate and higher permeability station, respectively. This is similar to the contribution of DNRA in intertidal permeable sediments

(Marchant et al. 2014), but lower than in temperate diffusive sediments (An and Gardner 2002; Trimmer and Nicholls 2009; Koop-Jakobsen and Giblin 2010; Jantti and Hietanen 2012). There also seems to be a correlation between OCR and DNRA in permeable sediments, although it is not as strong as that between OCR and denitrification (Supporting Information Fig. S3). So far, this relationship has only been investigated in temperate, eutrophied sands. It remains to be seen whether similar background levels of DNRA are found in all permeable sediments, or whether differences in organic matter loading, nitrate concentrations and temperature affect the ratio of DNRA to denitrification in other permeable sediments.

Ammonia oxidation

We observed oxic ammonia oxidation occurring within the sediment at all three stations both with (Fig. 4) and without (Fig. 2a) addition of allylthiourea (ATU). ATU should have inhibited ammonia oxidation (Ginestet et al. 1998), however only halved the rates. Similar observations of incomplete inhibition by ATU have been made previously and might be attributed to the presence of ammonia oxidizing Archaea (Santoro et al. 2010; Santoro and Casciotti 2011), although we have no direct evidence this was the case in our study.

To date, ammonia oxidation has only been measured under advective conditions in permeable sediments from intertidal regions, where volumetric rates were an order of magnitude lower than those measured here (Marchant et al. 2014). However, ammonia oxidation measurements have been made in sandy sediments under diffusive conditions (*see* Blackburn and Henriksen 1983; Ward 2008 and references therein) and the rates from this study are in the upper range of those.

A modeling study has predicted that advection in permeable sediments might reduce the potential for benthic nitrification (Kessler et al. 2013). Kessler et al. (2013) hypothesized that advective porewater flow would limit the ammonium available to ammonia oxidizers, as ammonium produced in anoxic sediments would be returned directly to the water column rather than be made available to supply ammonia oxidation. Comparison of the amount of ammonium produced in situ by aerobic remineralization (calculated from OCR) and the volumetric ammonia oxidation rates indicated that enough ammonium would have been released to support our observed rates (Fig. 6). In addition to this, the occurrence of both DNRA and denitrification in the presence of oxygen would have provided further sources of ammonium. This indicates that previous reports of ammonia oxidation in sandy sediments made under diffusive conditions are more likely to be an underestimation than an overestimation, as advective flows increase oxygen availability and oxygen penetration depths, both of which enhance the potential for nitrification (Lohse et al. 1993; Jensen et al. 1994, 1996; Gihring et al. 2010).

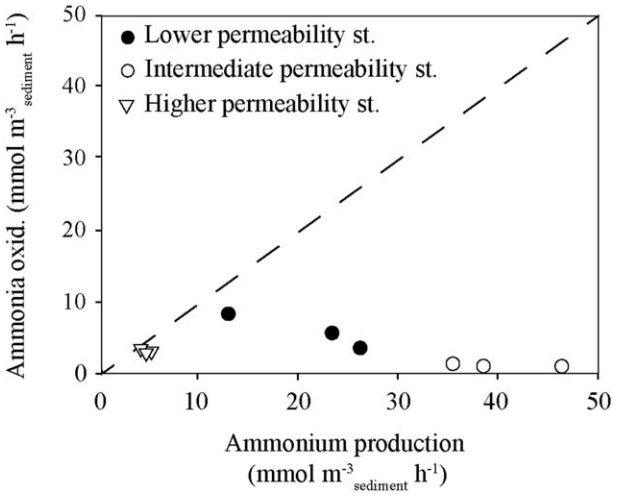

Fig. 6. Ammonium available to support ammonia oxidation. Ammonium production within the sediment was calculated from the aerobic remineralization of organic matter by oxygen respiration. The dashed line represents the maximum rate of ammonia oxidation that could be supported by the NH_4^+ produced within the sediment. As all points fall below the line, enough ammonium would have been available to support the measured rates at all stations.

It is interesting to note that of the two sets of ammonia oxidation rate measurements made so far under advective conditions in permeable sands, no generalizations can be made. Volumetric nitrification rates at a nearby intertidal location are consistently an order of magnitude lower than denitrification rates (Marchant et al. 2014), whereas in this study they were in the same range. Furthermore, in this study volumetric ammonia oxidation rates differed between each station, yet unlike denitrification did not correlate strongly with OCR (even though OCR could be described as a proxy for the amount of ammonia made available to support ammonia oxidation). Instead at the intermediate permeability station, where the highest OCR occurred, we observed the lowest ammonia oxidation rates. Therefore it appears that some other factor controls the potential for ammonia oxidation in permeable sediments—possibly competition for ammonia or other resources, such as surface area available for microbial colonization (Belser 1979) or oxygen availability (Henriksen et al. 1993).

Nitrite oxidation

Ammonia oxidation is generally considered as the rate limiting step for nitrification (e.g., Ward 2005) and the oxidation of nitrite as a separate process is often neglected. Our volumetric nitrite oxidation rates can currently only be considered as potential rates, as it is difficult to determine the robustness of the method we used due to the scarcity of previous measurements. It is possible that we underestimated the rates, as the co-occurrence of nitrate reduction (due to denitrification in the presence of oxygen) and ammonia oxidation during nitrite oxidation would have diluted the

$^{15}NO_2^-$ pool with $^{14}NO_2^-$ and, thus, lowered $^{15}NO_3^-$ production. We added high starting concentrations of $^{15}NO_2^-$ (100 μmol L^{-1}) to minimize the influence of such dilutions. This addition may have stimulated nitrite oxidation, in which case the nitrite oxidation rates would be overestimated. However, no evidence of stimulation of nitrite oxidation by the addition of NO_2^- has been observed previously in incubation experiments (Olson 1981; Clark et al. 2008). Our volumetric nitrite oxidation rates were consistently higher than ammonia oxidation rates, assuming that nitrite oxidation was not stimulated by the nitrite additions, this could suggests that the two processes were partly uncoupled in these sediments. A similar uncoupling of the two processes has been observed in suboxic ocean waters where nitrite oxidation and nitrate reduction co-occur (Füssel et al. 2011; Isobe et al. 2012).

N_2O production

Until recently subtidal permeable sediments were not assumed to be hotspots of nitrogen cycling and therefore they were rarely considered as a source of N_2O. While N_2O over saturations have been measured frequently in the water column throughout the North Sea (i.e., Law and Owens 1990), they are generally attributed to water column nitrification. We observed significant $^{15}N_2O$ formation in the $^{15}NH_4^+ + {}^{14}NO_x$ labeling experiment when oxygen was present and therefore concluded that oxic ammonia oxidation was the source. In the $^{15}NO_3^-$ experiment, $^{45+46}N_2O$ were produced both in the presence and absence of oxygen, indicating N_2O production from oxic and anoxic denitrification (Fig. 5a). The patterns of N_2O formation during denitrification observed at the lower and higher permeability stations are very similar to those in intertidal sandy sediments (unpubl. data). i.e., the ratio between N_2O and N_2 production was always higher during the oxic part of the incubation (Fig. 5b) and net N_2O consumption did not occur until nitrate became limiting (Supporting Information Fig. S2).

Coupled nitrification–denitrification

Coupled nitrification–denitrification is present in many diffusively dominated sediments, where it is separated spatially due to the occurrence of nitrification in upper oxic sediment layers and denitrification in lower anoxic layers (Jenkins and Kemp 1984). In these cases the extent of coupling is determined by the size of the nitrification zone and the diffusive transport of nitrate from the oxic layer to the deeper anoxic layer (for example as much as two thirds of nitrate diffuses upward into the water column (Meyer et al. 2008)). However, in permeable sediments, denitrification in the presence of oxygen as well as the advective transport of porewater within the sediment should allow much closer spatial and temporal coupling of the two processes.

Here, we observed very closely coupled nitrification–denitrification. When $^{15}NH_4^+$ was added to permeable sediments from the German Bight ($^{15}NH_4^+$ + ATU exp.), we observed a temporal overlap in nitrification and denitrification (Fig. 4; Supporting Information Fig. S4). In fact on addition of $^{15}NH_4^+$, the production of ^{15}N-N_2 by denitrification began almost concurrently with ammonia oxidation and nitrite oxidation. Between one and two thirds of the $^{15}NH_4^+$ in the $^{15}NH_4^+$ + ATU amendment experiment was already nitrified and subsequently denitrified before oxygen had been consumed. This indicates very close spatial coupling of nitrification and denitrification in the permeable sediments when they were oxic. Furthermore, as porewater ages and becomes anoxic on short time scales in the German Bight, temporal coupling between nitrification under oxic conditions and denitrification under anoxic conditions will also occur without the need for diffusive flux of nitrate. The combination of such closely coupled nitrification–denitrification and high nitrification rates means that this process has the potential to be a major path of N-loss in the German Bight, most likely leading to higher N-losses than previously estimated from nitrate fluxes alone.

Areal N-cycling rates

To estimate the impact of nitrification, denitrification, DNRA and the coupling between the processes on N-loss within the German Bight, it is necessary to upscale volumetric rates and examine areal rates. Generally in diffusive sediments, rates are integrated over the penetration depth of the appropriate solutes (e.g., oxygen in the case of nitrification, nitrate in the case of denitrification), which are determined from concentration profiles within the sediment. However in permeable sediments, advection plays a crucial role—flow paths of porewater start and end at the water-sediment-interface and are of different lengths. Therefore the penetration depth is a nonlinear function of time (Elliott and Brooks 1997b), which can be determined by modeling.

Using the approach of Elliott and Brooks (1997b) we calculated mean effective mixing depths for both O_2 and NO_3^- for all three stations. Oxygen penetrated into the sediment 7.5 mm, 7.7 mm, and 30 mm at the lower, intermediate and higher permeability stations respectively (Supporting Information Fig. S5). Such O_2 penetration depths are realistic in comparison to in situ measurements made during a subsequent cruise to the same region, providing validation of the model. However, areal rates are potentially underestimated when calculating effective mean mixing depths using advection as transport by molecular diffusion and porewater dispersion is neglected. Despite this, areal oxygen consumption rates calculated from the model were in the same range as those measured in situ previously using an autonomous benthic chamber with controlled advective porewater exchange (Janssen et al. 2005). Furthermore, while the areal nitrification rates spanned a large range (Table 3), they are of the same magnitude as previous areal nitrification estimates from continental shelf sediments e.g., 2.8 mmol m^{-2} d^{-1} (Laursen and Seitzinger 2002).

At all stations nitrate penetrated deeper than oxygen, to 12.2 mm, 11.1 mm, and 53 mm respectively, therefore there

was a layer of between 4 mm and 23 mm in which denitrification and DNRA could occur at their maximal rate. Here the important influence of coupled nitrification–denitrification within the sediment becomes apparent. Nitrification rates at the lower and higher permeability station exceeded oxic denitrification and DNRA rates, which meant that by the time the sediment became anoxic, nitrate concentrations were almost 1.5 times higher than the initial bottom water concentrations. This highlights the role that nitrification plays in sustaining N-loss in these sediments, as when bottom water concentrations of nitrate are low within the German Bight, e.g., in July when this study was carried out, extensive N-loss can still occur.

Nitrate concentrations are at their lowest in the German Bight during summer. In almost all other seasons, nitrate concentrations are higher than the 6–8 μmol L^{-1} measured in this study. This would have a number of consequences; first N-loss would increase. For example, increasing the bottom water nitrate concentration in the model to 35 μmol L^{-1} (a typical January concentration for this area (Dähnke et al. 2010)) would lead to a doubling in N-loss to 110 μmol N m^{-2} h^{-1}. Second, the impact of coupled nitrification–denitrification would be less pronounced, in the same winter scenario, only 45% of the nitrate required could be supplied by nitrification. Furthermore, as we did not sample in a prominent bloom or riverine run-off influenced season, organic matter (OM) concentrations were also likely to be comparatively low. Increases in organic matter concentrations would increase volumetric oxygen consumption and denitrification rates (*see* N-loss section), which has the effect of decreasing penetration depths calculated by the model, but still leading to higher areal N-loss rates.

It is therefore apparent that the highly permeable sediments we studied here have the potential to remove a significant amount of the atmospheric deposition and riverine fluxes of N to the German Bight. The important role of benthic nitrification in these sediments, which is closely coupled both spatially and temporally to denitrification means that significantly greater N-losses occur than would be expected from nitrate fluxes alone, especially in the periods of high primary production where nitrate concentrations are low. We can conclude therefore that the highly permeable subtidal sediments of the German Bight should also be considered as hotspots of N-cycling. Considering the strong relationship that is starting to emerge between OCR and volumetric denitrification rates in sandy sediments, it is becoming apparent that they likely provide a large sink for N that seems to be proportional to the increased inputs of nitrate and organic matter resulting from anthropogenic activity.

References

Ahmerkamp, S., C. Winter, F. Janssen, M. M. M. Kuypers, and M. Holtappels. 2015. The impact of bedform migration on benthic oxygen fluxes. J. Geophys. Res. Biogeosci. **120**: 2229–2242, doi:10.1002/2015JG003106

An, S. M., and W. S. Gardner. 2002. Dissimilatory nitrate reduction to ammonium (DNRA) as a nitrogen link, versus denitrification as a sink in a shallow estuary (Laguna Madre/Baffin Bay, Texas). Mar. Ecol. Prog. Ser. **237**: 41–50, doi:10.3354/meps237041.

Beddig, S., and others. 1997. Nitrogen fluxes in the German Bight. Mar. Pollut. Bull. **34**: 382–394. doi:10.1016/S0025-326X(96)00159-2

Belser, L. W. 1979. Population ecology of nitrfiying bacteria. Annu. Rev. Microbiol. **33**: 309–333. doi:10.1146/annurev.mi.33.100179.001521

Blackburn, T. H., and K. Henriksen. 1983. Nitrogen cycling in different types of sediments from Danish waters. Limnol. Oceanogr. **28**: 477–493. doi:10.4319/lo.1983.28.3.0477

Blott, S. J., and K. Pye. 2001. GRADISTAT: A grain size distribution and statistics package for the analysis of unconsolidated sediments. Earth Surf. Process. Landforms **26**: 1237–1248. doi:10.1002/esp.261

Braman, R. S., and S. A. Hendrix. 1989. Nanogram nitrite and nitrate determination in environmental and biological materials by vanadium(III) reduction with chemiluminescence detection. Anal. Chem. **61**: 2715–2718. doi:10.1021/ac00199a007

Canion, A., and others. 2014. Temperature response of denitrification and anammox reveals the adaptation of microbial communities to in situ temperatures in permeable marine sediments that span 50° in latitude. Biogeosciences **11**: 309–320, doi:10.5194/bg-11-309-2014.

Clark, D. R., A. P. Rees, and I. Joint. 2008. Ammonium regeneration and nitrification rates in the oligotrophic Atlantic Ocean: Implications for new production estimates. Limnol. Oceanogr. **53**: 52–62. doi:10.4319/lo.2008.53.1.0052

Cook, P. L. M., F. Wenzhofer, R. N. Glud, F. Janssen, and M. Huettel. 2007. Benthic solute exchange and carbon mineralization in two shallow subtidal sandy sediments: Effect of advective pore-water exchange. Limnol. Oceanogr. **52**: 1943–1963. doi:10.4319/lo.2007.52.5.1943

Dähnke, K., K. Emeis, A. Johannsen, and B. Nagel. 2010. Stable isotope composition and turnover of nitrate in the German Bight. Mar. Ecol. Prog. Ser. **408**: 7-U6, doi:10.3354/meps08558.

de Beer, D., and others. 2005. Transport and mineralization rates in North Sea sandy intertidal sediments, Sylt-Romo Basin, Wadden Sea. Limnol. Oceanogr. **50**: 113–127. doi:10.4319/lo.2005.50.1.0113

Devol, A. H., L. A. Codispoti, and J. P. Christensen. 1997. Summer and winter denitrification rates in western Arctic shelf sediments. Cont. Shelf Res. **17**: 1029–1033. doi:10.1016/S0278-4343(97)00003-4

Elliott, A. H., and N. H. Brooks. 1997a. Transfer of nonsorbing solutes to a streambed with bed forms: Laboratory experiments. Water Resour. Res. **33**: 137–151, doi:10.1029/96WR02783.

Elliott, A. H., and N. H. Brooks. 1997b. Transfer of nonsorbing solutes to a streambed with bed forms; Theory. Water Resour. Res. **33**: 123–136, doi:10.1029/96WR02784.

Emery, K. O. 1968. Relict sediments on continental shelves of world. AAPG Bull. **52**: 445–464.

Evrard, V., R. N. Glud, and P. L. Cook. 2013. The kinetics of denitrification in permeable sediments. Biogeochemistry **113**: 563–572. doi:10.1007/s10533-012-9789-x

Füssel, J., P. Lam, G. Lavik, M. M. Jensen, M. Holtappels, M. Gunter, and M. M. M. Kuypers. 2011. Nitrite oxidation in the Namibian oxygen minimum zone. ISME J. **6**: 1200–1209. doi:10.1038/ismej.2011.178

Gao, H., and others. 2010. Aerobic denitrification in permeable Wadden Sea sediments. ISME J. **4**: 417–426. doi:10.1038/ismej.2009.127

Gao, H., and others. 2012. Intensive and extensive nitrogen loss from intertidal permeable sediments of the Wadden Sea. Limnol. Oceanogr. **57**: 185–198, doi:10.4319/lo.2012.57.1.0185.

Gihring, T. M., A. Canion, A. Riggs, M. Huettel, and J. E. Kostka. 2010. Denitrification in shallow, sublittoral Gulf of Mexico permeable sediments. Limnol. Oceanogr. **55**: 43–54. doi:10.4319/lo.2010.55.1.0043

Ginestet, P., J. M. Audic, V. Urbain, and J. C. Block. 1998. Estimation of nitrifying bacterial activities by measuring oxygen uptake in the presence of the metabolic inhibitors allylthiourea and azide. Appl. Environ. Microbiol. **64**: 2266–2268.

Glud, R. N. 2008. Oxygen dynamics of marine sediments. Mar. Biol. Res. **4**: 243–289. doi:10.1080/17451000801888726

Gruber, N., and J. N. Galloway. 2008. An Earth-system perspective of the global nitrogen cycle. Nature **451**: 293–296. doi:10.1038/nature06592

Guo, H., J. Zhou, J. Su, and Z. Zhang. 2005. Integration of nitrification and denitrification in airlift bioreactor. Biochem. Eng. J. **23**: 57–62. doi:10.1016/j.bej.2004.05.010

Henriksen, K., T. H. Blackburn, B. A. Lomstein, and C. P. Mcroy. 1993. Rates of nitrification, distribution of nitrifying bacteria and inorganic N fluxes in northern Bering-Chukchi shelf sediments. Cont. Shelf Res. **13**: 629–651. doi:10.1016/0278-4343(93)90097-H

Holtappels, M., G. Lavik, M. M. Jensen, and M. M. M. Kuypers. 2011. ^{15}N-labeling experiments to dissect the contributions of heterotrophic denitrification and anammox to nitrogen removal in the OMZ waters of the ocean, p. 223–251. *In* M. G. Klotz [ed.], Methods in enzymology, Publisher, Elsevier.

Huettel, M., W. Ziebis, and S. Forster. 1996. Flow-induced uptake of particulate matter in permeable sediments. Limnol. Oceanogr. **41**: 309–322. doi:10.4319/lo.1996.41.2.0309

Huettel, M., H. Roy, E. Precht, and S. Ehrenhauss. 2003. Hydrodynamical impact on biogeochemical processes in aquatic sediments. Hydrobiologia **494**: 231–236. doi:10.1023/A:1025426601773

Huettel, M., P. Berg, and J. E. Kostka. 2014. Benthic exchange and biogeochemical cycling in permeable sediments. Ann. Rev. Mar. Sci. **6**: 23–51. doi:10.1146/annurev-marine-051413-012706

Isobe, K., and others. 2012. Nitrite transformations in an N-saturated forest soil. Soil Biol. Biochem. **52**: 61–63. doi:10.1016/j.soilbio.2012.04.006

Janssen, F., M. Huettel, and U. Witte. 2005. Pore-water advection and solute fluxes in permeable marine sediments (II): Benthic respiration at three sandy sites with different permeabilities (German Bight, North Sea). Limnol. Oceanogr. **50**: 779–792. doi:10.4319/lo.2005.50.3.0779

Jantti, H., and S. Hietanen. 2012. The effects of hypoxia on sediment nitrogen cycling in the Baltic Sea. Ambio **41**: 161–169. doi:10.1007/s13280-011-0233-6

Jenkins, M. C., and W. M. Kemp. 1984. The coupling of nitrification and denitrification in two estuarine sediments1, 2. Limnol. Oceanogr. **29**: 609–619. doi:10.4319/lo.1984.29.3.0609

Jensen, K. M, N. P. Sloth, N. Risgaard-Petersen, S. Rysgaard, and N. P. Revsbech. 1994. Estimation of nitrification and denitrification from microprofiles of oxygen and nitrate in model systems. Appl. Environ. Microbiol. **60**: 2094–2100. doi:10.4319/lo.1994.39.7.1643

Jensen, K. M., M. H. Jensen, and E. Kristensen. 1996. Nitrification and denitrification in Wadden Sea sediments (Konigshafen, Island of Sylt, Germany) as measured by nitrogen isotope pairing and isotope dilution. Aquat. Microb. Ecol. **11**: 181–191. doi:10.3354/ame011181

Jensen, M. M., B. Thamdrup, and T. Dalsgaard. 2007. Effects of specific inhibitors on anammox and denitrification in marine sediments. Appl. Environ. Microbiol. **73**: 3151–3158. doi:10.1128/AEM.01898-06

Jørgensen, B. B. 1982. Mineralization of organic matter in the sea bed—the role of sulphate reduction. Nature **296**: 643–645, doi:10.1038/296643a0.

Kessler, A. J., R. N. Glud, M. B. Cardenas, and P. L. Cook. 2013. Transport zonation limits coupled nitrification-denitrification in permeable sediments. Environ. Sci. Technol. **47**: 13404–13411. doi:10.1021/es403318x

Koop-Jakobsen, K., and A. E. Giblin. 2010. The effect of increased nitrate loading on nitrate reduction via denitrification and DNRA in salt marsh sediments. Limnol. Oceanogr. **55**: 789–802. doi:10.4319/lo.2009.55.2.0789

Laursen, A. E., and S. P. Seitzinger. 2002. The role of denitrification in nitrogen removal and carbon mineralization in Mid-Atlantic Bight sediments. Cont. Shelf Res. **22**: 1397–1416. doi:10.1016/S0278-4343(02)00008-0

Law, C. S., and N. J. P. Owens. 1990. Denitrification and nitrous oxide in the North Sea. Neth. J. Sea Res. **25**: 65–74. doi:10.1016/0077-7579(90)90009-6

Lohse, L., J. F. P. Malschaert, C. P. Slomp, W. Helder, and W. Van Raaphorst. 1993. Nitrogen cycling in North Sea sediments: Interaction of denitrification and nitrification in

offshore and coastal areas. Mar. Ecol. Prog. Ser. **101**: 283–283. doi:10.3354/meps101283

Marchant, H. K., G. Lavik, M. Holtappels, and M. M. M. Kuypers. 2014. The fate of nitrate in intertidal permeable sediments. PloS one **9**: e104517. doi:10.1371/journal.pone.0104517

Meyer, R. L., D. E. Allen, and S. Schmidt. 2008. Nitrification and denitrification as sources of sediment nitrous oxide production: A microsensor approach. Mar. Chem. **110**: 68–76. doi:10.1016/j.marchem.2008.02.004

Münch, E. V., P. Lant, and J. Keller. 1996. Simultaneous nitrification and denitrification in bench-scale sequencing batch reactors. Water Res. **30**: 277–284, doi:10.1016/0043-1354(95)00174-3.

Nielsen, L. P. 1992. Denitrification in sediment determined from nitrogen isotope pairing. FEMS Microbiol. Ecol. **86**: 357–362. doi:10.1016/0378-1097(92)90800-4

Olson, R. J. 1981. 15-N tracer studies of the primary nitrite maximum. J. Mar. Res. **39**: 203–226.

Paetsch, J., A. Serna, K. Daehnke, T. Schlarbaum, A. Johannsen, and K.-C. Emeis. 2010. Nitrogen cycling in the German Bight (SE North Sea)—clues from modelling stable nitrogen isotopes. Cont. Shelf Res. **30**: 203–213. doi:10.1016/j.csr.2010.06.010

Polerecky, L., U. Franke, U. Werner, B. Grunwald, and D. De Beer. 2005. High spatial resolution measurement of oxygen consumption rates in permeable sediments. Limnol. Oceanogr.: Methods **3**: 75–85. doi:10.4319/lom.2005.3.75

Prakasam, T. B. S., and R. C. Loehr. 1972. Microbial nitrification and denitrification in concentrated wastes. Water Res. **6**: 859–869. doi:10.1016/0043-1354(72)90038-3

Preisler, A., D. De Beer, A. Lichtschlag, G. Lavik, A. Boetius, and B. B. Jørgensen. 2007. Biological and chemical sulfide oxidation in a Beggiatoa inhabited marine sediment. ISME J. **1**: 341–353. doi:10.1038/ismej.2007.50

Rabalais, N. N. 2002. Nitrogen in aquatic ecosystems. Ambio **31**: 102–112. doi:10.1579/0044-7447-31.2.102

Rao, A. M. F., M. J. Mccarthy, W. S. Gardner, and R. A. Jahnke. 2007. Respiration and denitrification in permeable continental shelf deposits on the South Atlantic Bight: Rates of carbon and nitrogen cycling from sediment column experiments. Cont. Shelf Res. **27**: 1801–1819. doi:10.1016/j.csr.2007.03.001

Rao, A. M. F., M. J. Mccarthy, W. S. Gardner, and R. A. Jahnke. 2008. Respiration and denitrification in permeable continental shelf deposits on the South Atlantic Bight: N_2: Ar and isotope pairing measurements in sediment column experiments. Cont. Shelf Res. **28**: 602–613, doi:10.1016/j.csr.2007.11.007.

Revsbech, N. P. 1989. An oxygen microsensor with a guard cathode. Limnol. Oceanogr. **34**: 474–478, doi:10.4319/lo.1989.34.2.0474

Rocha, C., S. Forster, E. Koning, and E. Epping. 2005. High-resolution permeability determination and two-dimensional porewater flow in sandy sediment. Limnol. Oceanogr.: Methods **3**: 10–23. doi:10.4319/lom.2005.3.10

Santoro, A. E., K. L. Casciotti, and C. A. Francis. 2010. Activity, abundance and diversity of nitrifying archaea and bacteria in the central California Current. Environ. Microbiol. **12**: 1989–2006. doi:10.1111/j.1462-2920.2010.02205.x

Santoro, A. E., and K. L. Casciotti. 2011. Enrichment and characterization of ammonia-oxidizing archaea from the open ocean: Phylogeny, physiology and stable isotope fractionation. ISME J. **5**: 1796–1808. doi:10.1038/ismej.2011.58

Sharma, B., and R. C. Ahlert. 1977. Nitrification and nitrogen removal. Water Res. **11**: 897–925. doi:10.1016/0043-1354(77)90078-1

Sokoll, S., M. Holtappels, P. Lam, G. Collins, M. Schluter, G. Lavik, and M. M. M. Kuypers. 2012. Benthic nitrogen loss in the arabian sea off pakistan. Front. Microbiol. **3**: 395–395. doi:10.3389/fmicb.2012.00395

Song, G. D., S. M. Liu, H. Marchant, M. M. M. Kuypers, and G. Lavik. 2013. Anammox, denitrification and dissimilatory nitrate reduction to ammonium in the East China Sea sediment. Biogeosciences **10**: 6851–6864. doi:10.5194/bg-10-6851-2013

Tait, D. R., D. V. Erler, A. Dakers, L. Davison, and B. D. Eyre. 2013. Nutrient processing in a novel on-site wastewater treatment system designed for permeable carbonate sand environments. Ecol. Eng. **57**: 413–421. doi:10.1016/j.ecoleng.2013.04.027

Thamdrup, B., and D. E. Canfield. 1996. Pathways of carbon oxidation in continental margin sediments off central Chile. Limnol. Oceanogr. **41**: 1629–1650. doi:10.4319/lo.1996.41.8.1629

Thamdrup, B., and T. Dalsgaard. 2002. Production of N_2 through anaerobic ammonium oxidation coupled to nitrate reduction in marine sediments. Appl. Environ. Microbiol. **68**: 1312–1318. doi:10.1128/AEM.68.3.1312-1318.2002

Thibodeaux, L. J., and J. D. Boyle. 1987. Bedform-generated convective transport in bottom sediment. Nature **325**: 341–343. doi:10.1038/325341a0

Trimmer, M., and J. C. Nicholls. 2009. Production of nitrogen gas via anammox and denitrification in intact sediment cores along a continental shelf to slope transect in the North Atlantic. Limnol. Oceanogr. **54**: 577–589. doi:10.4319/lo.2009.54.2.0577

Van Beusekom, J. E. E. 2005. A historic perspective on Wadden Sea eutrophication. Helgol. Mar. Res. **59**: 45–54. doi:10.1007/s10152-004-0206-2

Van Beusekom, J. E. E., M. Loebl, and P. Martens. 2009. Distant riverine nutrient supply and local temperature drive the long-term phytoplankton development in a temperate coastal basin. J. Sea Res. **61**: 26–33. doi:10.1016/j.seares.2008.06.005

Ward, B. B. 2005. Temporal variability in nitrification rates and related biogeochemical factors in Monterey Bay,

California, USA. Mar. Ecol. Prog. Ser. **292**: 97–109. doi: 10.3354/meps292097

Ward, B. B. 2008. Nitrification in Marine Systems. Nitrogen in the marine environment, p. 199–261. *In* D. G. Capone, D. A. Bronk, M. R. Mulholland, and E. J. Carpenter [eds]. Academic Press.

Waremburg, F. 1993. Nitrogen fixation in soil and plant systems, p. 157–180. *In* K. B. T. Knowles [ed.], Nitrogen isotopes techniques. Academic Press.

Yoo, H., K. H. Ahn, H. J. Lee, K. H. Lee, Y. J. Kwak, and K. G. Song. 1999. Nitrogen removal from synthetic wastewater by simultaneous nitrification and denitrification (SND) via nitrite in an intermittently-aerated reactor. Water Res. **33**: 145–154. doi:10.1016/S0043-1354(98)00159-6

Acknowledgments

We sincerely thank cruise leader Thomas Lüdmann as well as the captain and crew of the R.V. *Heincke* (HE-383). We are grateful to Gabi Klockgether and Sarah Kuschnerow for technical assistance. We also thank Felix Janssen with whom discussion helped improve the manuscript. Furthermore we thank two anonymous reviewers whose comments greatly improved the manuscript. This work was financially supported by the Max Planck Society and the DFG-Research Center/ Cluster of Excellence ''The Ocean in the Earth System'' at the University of Bremen.

Submitted 20 February 2015
Revised 10 August 2015; 1 December 2015; 7 January 2016
Accepted 9 January 2016

Associate editor: Bo Thamdrup